

Performance Degradation in Cooperative Radar Sensor Systems due to Uncorrelated Phase Noise

Andreas Frischen*, Juergen Hasch*, and Christian Waldschmidt†

*Robert Bosch GmbH, Corporate Sector Research and Advance Engineering, P.O. Box 10 60 50, D-70049 Stuttgart, Germany

†Institute of Microwave Techniques, Ulm University, Albert-Einstein-Allee 41, D-89081 Ulm, Germany

Email: {andreas.frischen, juergen.hasch}@de.bosch.com, christian.waldschmidt@uni-ulm.de

Abstract—A cooperative radar sensor system consists of two or more radar sensors, which are capable of mutually receiving the target responses (cross echoes) of the transmitted signals. The sensors have individual signal sources, that are used both for transmission and reception. In addition to the non-ideal properties of single sensors, the usage of different signal sources for transmission and reception in each path leads to uncorrelated phase noise. In this paper, its influence on target position estimation is investigated. An in-system measurement methodology is proposed, which allows to evaluate the effect isolated and to derive phase-noise performance requirements for component design. In the system setup, the signal sources of the radar sensors are represented by an arbitrary-waveform generator (AWG). By this means, both ideally coherent and perturbed sensor signals can be generated for measurements. Starting from the evaluation of phase-noise-free signals, the degradation in target position estimation performance under the influence of phase noise is evaluated in measurements and compared to simulation results.

I. INTRODUCTION

Multiple Input Multiple Output (MIMO) Radar Systems have gained increasing interest within the last years. Their capability to determine target positions at high precision using a relatively small number of total channels makes them attractive for cost-sensitive, yet high-accuracy demanding applications. MIMO radar systems can be distinguished between systems with colocated and widely-separated antennas. While the former approach features a coherent processing gain and therefore high angular resolution, it is prone to target fading[1]. In contrast, widely-separated antennas do not offer a coherent processing gain, but provide a better exploitation of spatial diversity. The main advantages of a system with widely-separated antennas include its tolerance to radar-cross-section (RCS) variations and the avoidance of problems with ghost targets in multi-target scenarios[2]. It has been shown that MIMO techniques can be implemented with several low-complexity radar units by a cooperative radar approach[3].

In this work, the performance of a radar system consisting of distributed individual sensors with cooperative processing of cross-echo signals is evaluated under the influence of phase noise in the radar signals. A methodology is provided to specify phase-noise requirements for component design by system performance evaluations. The proposed approach allows measurements in real environments or crucial scenarios. It is applied to a cooperative radar sensor system, in which the phase noise of the signal sources has an exceedingly high influence on the target detection performance of the system.

The paper is structured as follows. Section II introduces the cooperative radar system which is the subject of this

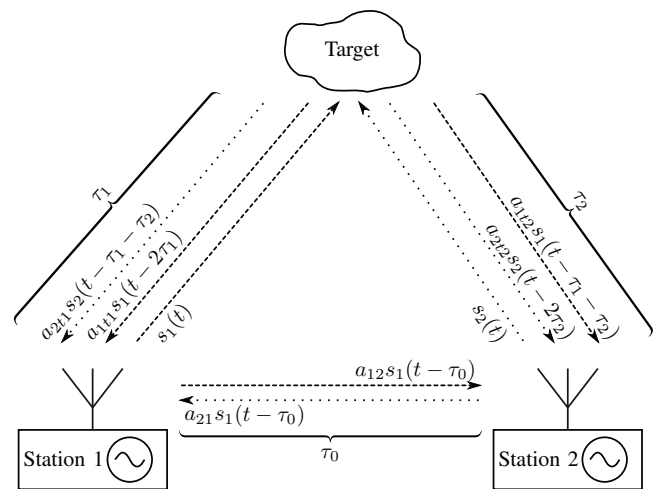


Fig. 1. Composition of received signals in a cooperative radar sensor system

examination. In section III, an analytical signal model for the received signal is developed. The phase noise model that was derived by Demir et al. in [4] is applied to the signal model and the influence on target position estimation performance is evaluated. In section IV, a measurement setup which allows the incorporation of a defined amount of phase noise in the signal sources is proposed. The simulation and measurement results are presented in section V. Section VI concludes the paper.

II. COOPERATIVE OPERATION PRINCIPLE

The examined system consists of two frequency-modulated continuous-wave (FMCW) radars, both transmitting frequency ramps with a certain frequency offset Δf . The stations receive the target response from their own and the respective other transmitted wave, whereby the latter is shifted by the offset Δf in the frequency domain. In the following, these two components will be referred to as monostatic and bistatic radar response, respectively. A third component occurs due to the direct coupling of the two stations. The composition of the received signal is summarized in Fig. 1.

While the monostatic response can be processed using traditional techniques [5], the bistatic response introduces additional information compared to single-sensor measurements. A method for the processing of secondary radar signals to determine the distance between two stations has been introduced in [6]. An approach to process the bistatic response

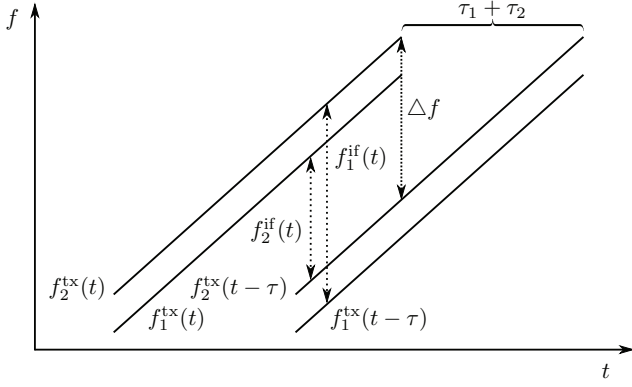


Fig. 2. Bistatic radar responses in the frequency domain

in a cooperative secondary radar with two loosely-coupled stations was presented in [3]. A key factor for the achievable performance is the phase noise, as will be pointed out in section III.

In Fig. 2, the transmit signals of the two stations and radar responses of a single target are depicted in the frequency domain, assuming a configuration corresponding to Fig. 1. The time of flight $\tau_1 + \tau_2$ leads to a beat frequency, which is superimposed by the frequency offset Δf . Note that, for illustrative purposes, the frequency shifts in Fig. 2 are not proportional. In reality, the resulting frequencies $f_m^{if}(t)$ are dominated by the frequency shift Δf , which is necessary to guarantee that the monostatic and bistatic responses can be separated in the frequency domain.

III. MATHEMATICAL SIGNAL MODEL

A. Cooperative Radar Signal Model

Consider an arrangement according to Fig. 1. The positions of the M sensors and the target are denoted as p_m , $m \in \{1 \dots M\}$ and p_t , respectively.

$$p_m = \begin{pmatrix} p_{m,x} \\ p_{m,y} \\ p_{m,z} \end{pmatrix}, p_t = \begin{pmatrix} p_{t,x} \\ p_{t,y} \\ p_{t,z} \end{pmatrix}. \quad (1)$$

Each sensor transmits an FMCW ramp signal.

$$s_m(t) = \exp(j2\pi f_m t) \exp(j(\pi k_{r,m} t^2 + \phi_{0,m}(t))) \quad (2)$$

Here, $k_{r,m} = \frac{f_{bw}}{T_{mod}} + k_{r,m}^{offset} = k_r + k_{r,m}^{offset}$ denotes the respective slope, where f_{bw} represents the bandwidth and T_{mod} the modulation time of the ramp. $\phi_{0,m}(t)$ refers to a time-dependent phase fluctuation representing the phase noise of the respective oscillator. At the same time, every sensor receives both the transmitted signal from itself and from all other sensors.

$$r_m(t) = \sum_{n=1}^M a_{ntm} \cdot s_n(t - \tau_{ntm}) \quad (3)$$

Here, τ_{ntm} is the travel time of the signal from sensor n to target t and further to sensor m . For static scenarios, it is a time-invariant variable depending on the receiver position p_m ,

the transmitter position p_n , the target position p_t , and the phase velocity c .

$$\tau_{ntm} = \frac{|p_m - p_t| + |p_t - p_n|}{c} \quad (4)$$

Each sensor converts the received signal to baseband by mixing it with its own (complex conjugate) transmit signal.

$$r_{m,bb}(t) = r_m(t) s_m^*(t) \quad (5)$$

Considering only the bistatic response of an arrangement with $M = 2$ sensors, the baseband signal at station m receiving the radar response from target t of the transmit signal from station n , $(m, n) \in \{(1, 2), (2, 1)\}$ becomes

$$r_{m,bb}^{bistat}(t) = a_{ntm} \exp \left(j \left(2\pi(f_n - f_m)t - 2\pi f_n \tau_{ntm} - 2\pi k_r \tau_{ntm} t + \pi k_r \tau_{ntm}^2 + \phi_{0,m}(t) - \phi_{0,n}(t - \tau_{ntm}) \right) \right) \quad (6)$$

B. Phase-Noise Modeling

Several methods for phase noise modeling and prediction from simulations have been presented in the past [7], [8], [4]. In this work, the used phase noise model is based on the work in [4]. Some of the findings, that are used in our signal model, are recapitulated in the following.

- 1) The output $x_s(t)$ of an oscillator is perturbed to $x_s(t + \alpha(t)) + y(t)$, where $\alpha(t)$ represents a phase shift in the periodic output that grows over time, while $y(t)$ represents an additive term that remains small.
- 2) The phase fluctuation described by $\alpha(t)$ is a stationary stochastic process leading to
 - a) a mean square jitter increasing linearly in time, characterized by a scalar constant c_{pn}
 - b) a constant cycle-to-cycle jitter
- 3) $\alpha(t)$ becomes a Gaussian random variable, asymptotically with time

For large times t , the expectation $E[\alpha(t)\alpha(t + \tau)]$ shows to be

$$E[\alpha(t)\alpha(t + \tau)] = m^2 + c_{pn} \cdot \min(t, t + \tau) \quad (7)$$

with $m = \mu(t)$ and

$$c_{pn} \cdot t = \sigma^2(t). \quad (8)$$

$\mu(t)$ is the time-dependent mean of the phase fluctuations which settles to the final value m for large times t [4]. Focussing on the phase fluctuations in the stationary case, the influence of $\mu(t)$ is neglected, as a constant frequency offset can easily be compensated. $\sigma^2(t)$ corresponds to the variance of the random process $\alpha(t)$. Statement 2b together with equation 8 can be used to generate phase noise perturbations in the time-domain.

In equation 2, the phase noise was already considered by the term $\phi_{0,m}(t)$. In order to match the introduced phase noise model, it has to be set to

$$\phi_{0,m}(t) = 2\pi f_m \alpha_m(t) \quad (9)$$

with α_m representing the random process of the phase noise of oscillator m . Implicitly, the phase noise is only modeled for the carrier at the frequency f_m , while the impact of the phase noise added by the modulation is not subject of the

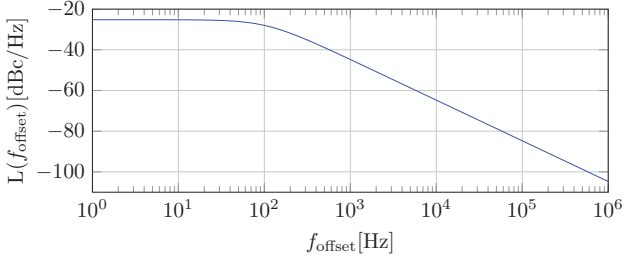


Fig. 3. Power density of phase noise with parameter $c_{pn} = 10^{-18} \text{ s}^2\text{Hz}$

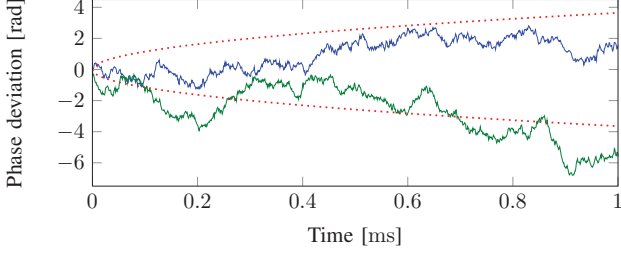


Fig. 4. Two realizations of phase deviation random walks

examination. Note that the phase noise model in [4] has some limitations, such as the missing incorporation of $1/f$ noise. In systems where phase noise close to the carrier is significant, an appropriate model has to be chosen. The power density of the phase noise is given by equation (41) in [4] and exemplarily illustrated in Fig. 3 for $c_{pn} = 10^{-18} \text{ s}^2\text{Hz}$ and $f_0 = 5.8 \text{ GHz}$.

C. Signal Processing

An approach to process the IF signals of both stations was introduced in [3]. Its main idea is to process both signals in a central unit, which allows the separation of target object responses from the effects due to imperfect synchronization.

Equation 10 in [3] can then be applied to the two received bistatic spectral parts and peak-detection performed on the resulting combined spectrum. While a constant phase offset is considered in the aforementioned work and the signal processing therein, phase noise was not subject of that contribution.

Figure 4 shows two realizations of random walks (solid lines) representing the occurring phase deviations due to phase noise for a fundamental frequency of $f_0 = 5.8 \text{ GHz}$ and the phase noise parameter $c_{pn} = 10^{-18} \text{ s}^2\text{Hz}$. It can be interpreted as the phase noise $\phi_{0,1}(t)$ and $\phi_{0,2}(t)$ of two independent signal sources and thereby illustrates the impact of uncorrelated phase noise on cooperative radar sensor systems. As long as the same signal source is used to generate the transmit signal and to down-convert the receive signal, the effective phase deviation in the baseband is determined by the difference in phase deviation of a single random walk realization for a time difference equal to the time of flight, e.g. $\phi_{\text{err}} = \phi_{0,1}(t) - \phi_{0,1}(t - \tau)$. In a cooperative radar sensor system, however, a different signal source is used to down-convert the transmit signal, so that the effective phase deviation in the baseband is determined by the difference in phase deviation of two random walk realizations and a time difference equal to the time of flight, e.g. $\phi_{\text{err}} = \phi_{0,2}(t) - \phi_{0,1}(t - \tau)$. Applying these equations to the depicted random walk realizations and

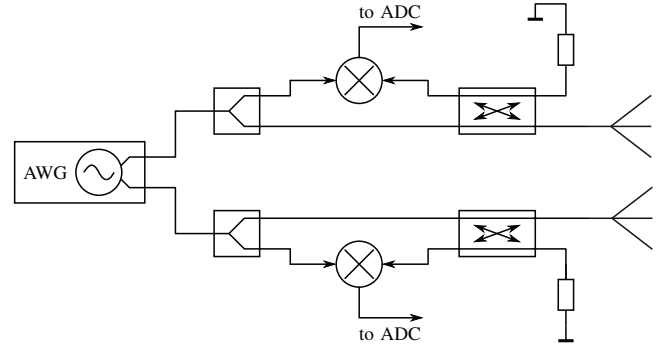


Fig. 5. Measurement setup with AWG signal generation

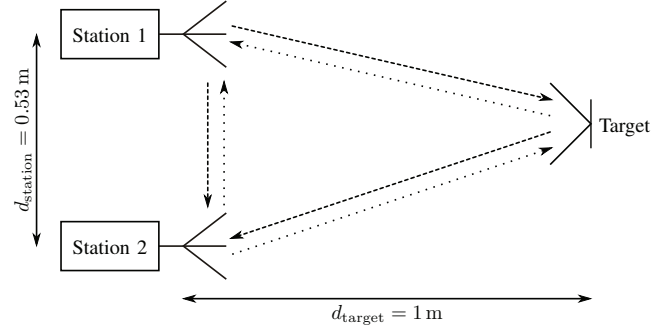


Fig. 6. Measurement scene with two stations and corner reflector

keeping in mind that typical time-of-flights are in the sub- μm range reveals that phase noise is particularly an issue for cooperative radar sensor systems. The dotted line in figure 4 represents the standard deviation $\sigma(t)$ according to equation 8 and is therefore an estimate of the expected phase deviation dependent on the total measurement time. As a consequence, shorter modulation times are advantageous in terms of total phase deviations.

IV. MEASUREMENT SETUP

In order to validate the findings in section III, a measurement setup has been developed that allows utilizing both ideal and non-ideal signals within the radar sensor stations. The block diagram of the setup is depicted in Fig. 5, where the upper and the lower half each represent one of the two stations. As the signals for both stations are generated with an AWG with two independent but coherent outputs, frequency ramps with specific phase noise power densities can be generated. The phase deviations are calculated beforehand and incorporated in the array of samples, which is repeated by the AWG.

The following power splitter directs the signal both to the station's Vivaldi antenna and to the LO input of the downconversion mixer. The received signal is led to the RF input of the mixer via a 10 dB coupler. The IF output of the mixer is then sampled and further processed in a PC. Additional amplifiers are used both in the high- and low-frequency domain, but omitted in Fig. 5 for simplicity.

Fig. 6 illustrates the measured scene. For the results in section V, a dihedral corner reflector was used as a target. Note that their reflection properties can be disadvantageous

TABLE I. MEASUREMENT PARAMETERS

Fundamental frequency	f_0	5.8 GHz
Frequency offset	Δf	500 kHz
Modulation bandwidth	f_{bw}	500 MHz
Modulation time	T_{mod}	1 ms
AWG sampling frequency	$f_{sample,AWG}$	25 GS/s
IF sampling frequency	$f_{sample,IF}$	2 MS/s
Number of IF samples	$N_{sample,IF}$	2000
Distance between stations	$d_{station}$	0.53 m
Target distance	d_{target}	1 m
Phase noise parameter	c_{pn}	$10^{-18} \text{ s}^2\text{Hz}$

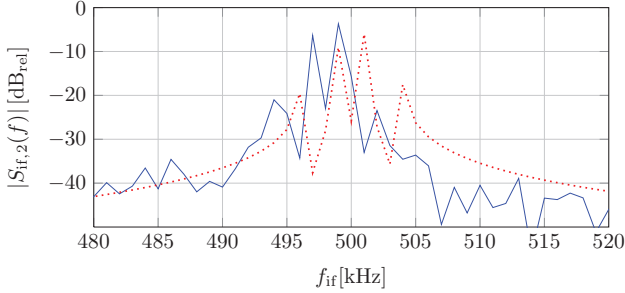


Fig. 7. Measured and simulated spectra near 500 kHz with clean signals

in bistatic measurements, depending on the angle between the transmit and receive station [9].

V. SIMULATION AND MEASUREMENT RESULTS

Table I summarizes the parameters of the simulations and measurements. The resulting IF spectra at station 2 near the frequency offset $\Delta f = 500$ kHz for unperturbed signals are depicted in Fig. 7 both for the simulation (dotted line) and measurement (solid line). The direct coupling has its peak at 497 kHz (measurement), corresponding to the distance between the stations $d_{station} = 0.53$ m, while the bistatic response has its peak at 494 kHz, corresponding to the total distance according to $d_{bistat} = 2\sqrt{\left(\frac{d_{station}}{2}\right)^2 + d_{target}^2} = 2.07$ m. The mirrored peaks occur due to real-valued (non-I/Q) mixing, while large signal paths in the discrete setup lead to an additional frequency offset in the measurements. Both paths can be separated and identified reliably due to the decrease in power density between these peaks at 496 kHz of about 14 dB. From the peak frequency difference the target signal path can be calculated to be approximately $\frac{3 \text{ kHz} \cdot c_0 \cdot T_{mod}}{f_{bw}} = 1.8$ m larger than the station distance. Interpolation techniques to improve the accuracy have been presented in [10].

In the second measurement, phase-noise-perturbed signals have been generated. Fig. 8 shows the same extract from the frequency spectrum of the IF signal of station 2 as before. The peaks were broadened by the phase noise, leading to a higher power density in between. The dynamic between the bistatic response and the local minimum decreased to less than 6 dB, making the separation and identification of the paths less reliable. At a target distance of 1 m, the phase-noise perturbed system already operates at its limit of performance. For even closer targets, the peaks of the two paths blur and cannot be separated.

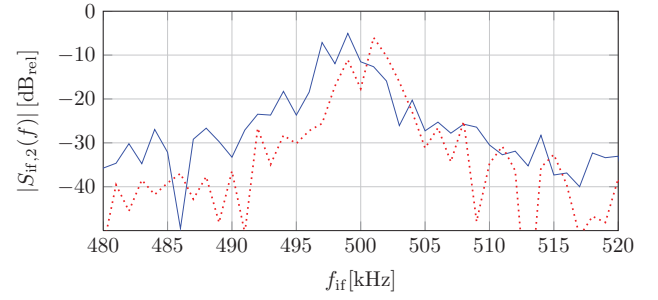


Fig. 8. Measured and simulated spectra near 500 kHz with phase-noise perturbed signals

VI. CONCLUSION

In this work, a hardware setup with two radar sensor stations was proposed, which allows the examination of the influence of phase noise on the performance of cooperative radar sensor systems. Since the signals of both stations were generated by an arbitrary waveform generator, any desired phase noise models could be implemented and used in the signals and measurements. A simple phase noise model based on the analytical studies in [4] was implemented and its impact on the cooperative radar system demonstrated. The proposed methodology allows to derive phase-noise requirements by measurements of critic scenarios, thus providing vital specifications for component design. In the exemplarily shown setup, the phase noise parameter c_{pn} of the oscillators may not exceed $c_{pn,max} = 10^{-18} \text{ s}^2\text{Hz}$. Otherwise, the system is not capable of detecting objects at distances of 1 m or less.

REFERENCES

- [1] E. Fishler, A. Haimovich, R. Blum, L. Cimini, D. Chizhik, and R. Valenzuela, "Spatial diversity in radars-models and detection performance," *IEEE Trans. Signal Process.*, vol. 54, no. 3, pp. 823–838, March 2006.
- [2] S. Kong, S. Lee, C.-Y. Kim, and S. Hong, "Wireless cooperative synchronization of coherent UWB MIMO radar," *IEEE Trans. Microw. Theory Tech.*, vol. 62, no. 1, pp. 154–165, Jan 2014.
- [3] R. Feger, C. Pfeffer, C. Schmid, M. J. Lang, Z. Tong, and A. Stelzer, "A 77-GHz FMCW MIMO radar based on loosely coupled stations," in *Microwave Conference (GeMiC), 2012 The 7th German*, March 2012, pp. 1–4.
- [4] A. Demir, A. Mehrotra, and J. Roychowdhury, "Phase noise in oscillators: a unifying theory and numerical methods for characterization," *IEEE Trans. Circuits Syst. I, Fundam. Theory Appl.*, vol. 47, no. 5, pp. 655–674, May 2000.
- [5] A. Carr, L. Cuthbert, and A. D. Olver, "Digital signal processing for target detection in FMCW radar," *Proc. IEEE Commun. Radar and Signal Process.*, vol. 128, no. 5, pp. 331–336, October 1981.
- [6] S. Roehr, M. Vossiek, and P. Gulden, "Method for high precision radar distance measurement and synchronization of wireless units," in *Microwave Symposium, 2007. IEEE/MTT-S International*, June 2007, pp. 1315–1318.
- [7] B. Razavi, "A study of phase noise in CMOS oscillators," *IEEE J. Solid-State Circuits*, vol. 31, no. 3, pp. 331–343, Mar 1996.
- [8] A. Hajimiri and T. Lee, "A general theory of phase noise in electrical oscillators," *IEEE J. Solid-State Circuits*, vol. 33, no. 2, pp. 179–194, Feb 1998.
- [9] J. Jackson, "Analytic physical optics solution for bistatic, 3d scattering from a dihedral corner reflector," *IEEE Trans. Antennas Propag.*, vol. 60, no. 3, pp. 1486–1495, March 2012.
- [10] D. Rife and R. Boorstyn, "Single tone parameter estimation from discrete-time observations," *IEEE Trans. Inf. Theory*, vol. 20, no. 5, pp. 591–598, Sep 1974.